Strong Nonlinear Response of Superconducting Tunnel Junctions due to Localized Traps

A. Poelaert,[1] A. G. Kozorezov,[2] A. Peacock,[1] and J. K. Wigmore[2]
[1]*Astrophysics Division, European Space Agency, ESTEC, Noordwijk, The Netherlands*
[2]*School of Physics and Chemistry, Lancaster University, Lancaster, United Kingdom*
(Received 25 June 1998)

The responsivity of a single superconducting tunnel junction for photon detection has been determined over a wide range of energy from optical to hard x ray. An unexpected rapid increase of responsivity is found in the ultraviolet regime. We show that the effect is due to the presence of localized traps—regions of locally reduced energy gap containing a number of confined states. The balance equations for nonequilibrium quasiparticles have been generalized to account for the effects of localized traps. Quantitative modeling yields the details of trap density and trapping probability. [S0031-9007(98)08375-6]

PACS numbers: 73.50.Gr, 74.40.+k, 74.50.+r, 85.25.–j

One of the most exciting recent developments in astrophysical instrumentation in recent years has been the use of superconducting tunnel junctions (STJ) to detect single photons at optical wavelengths [1]. In contrast to charge coupled devices, STJ's also possess intrinsic wavelength and time resolution, thus providing the basis for photon counting systems which are far superior to existing types. STJ's have previously been used to detect ultraviolet and x-ray photons [2], however the STJ responsivity at these energies is invariably larger than for optical photons. This unexpected result cannot be explained on the basis of the standard Rothwarf-Taylor description of nonequilibrium quasiparticle (qp) dynamics [3]. According to this model responsivity should decrease monotonically with increasing photon energy due to the increasing self-recombination [3,4]. In this paper we present detailed experimental results on the responsivity of a single STJ device over a wide range of energy, from the visible to the hard x-ray region (Fig. 1). The device used was a high quality epitaxially grown, Nb-Al-AlO_x-Al-Nb proximised structure which has enhanced responsivity due to multiple tunneling. We found that the responsivity remained constant throughout the optical and near ultraviolet range, then rose rapidly to a peak value of approximately 43 times the optical value, before falling nearly hyperbolically along the curve expected due to self-recombination. We shall show that the observed energy variation of these quantities is due to the presence of "pools" having reduced energy gap and giving rise to potential wells each containing a number of localized states in which the qp's may be confined. These will be referred to as localized traps. Our results suggest that the localized traps play no less a significant role in superconductors than in semiconductors.

Balance equations in the presence of localized trapping states.—To describe the time evolution of nonequilibrium qp's and the phonon distributions generated by the absorption of a photon in the STJ, the phenomenological Rothwarf-Taylor (RT) equations may be written (in the case where, due to fast phonon pair breaking, phonons remain in local equilibrium with qp's) [3,4]

$$\begin{aligned}\frac{dn_1}{dt} &= -\,n_1(\Gamma_{t,1} + \Gamma_{QL,1} + \Gamma_{QPL,12} + \Gamma_{QPL,1}) \\ &\quad + n_2(\Gamma_{t,2} + \Gamma_{QPL,21}) \\ \frac{dn_2}{dt} &= -\,n_2(\Gamma_{t,2} + \Gamma_{QL,2} + \Gamma_{QPL,21} + \Gamma_{QPL,2}) \\ &\quad + n_1(\Gamma_{t,1} + \Gamma_{QPL,12})\,.\end{aligned} \tag{1}$$

Here n_j and n_T are densities of nonequilibrium and thermal qp's in electrode j; $\Gamma_{t,j}$ is the tunnel rate from electrode j; and $\Gamma_{QPL,ji}$, $\Gamma_{QPL,j}$ are loss rates due to recombination. $\Gamma_{QPL,ji}$, corresponds to phonon escape from electrode j into i (phonon coupling) and $\Gamma_{QPL,j}$ accounts for phonon escape into surrounding materials (e.g., the substrate). It is given by $\Gamma_{QPL,j} = (n_j + 2n_T)R^*$ with the effective recombination coefficient R^*. Finally, $\Gamma_{QL,j}$ is the loss rate due to any process other than recombination, notably diffusion into leads and trapping by localized states. Because of the dependence of the recombination rate on qp density (self-recombination) Eqs. (1) are nonlinear. The measured

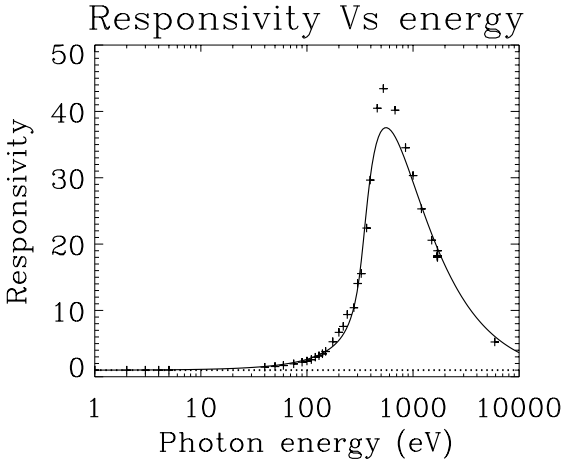

FIG. 1. The responsivity vs photon energy: data (+) together with the theoretical fit (solid line).

charge $Q(E)$, where E is the energy of the absorbed photon, is the integral over the total excess tunneling current and can be easily expressed in terms of the solution of Eqs. (1). We shall define a fundamental STJ responsivity $S(E)$ as $Q(E)$ per unit E normalized to the limit of an infinitesimally small E. Thus,

$$S(E) \equiv \frac{Q(E)}{E} \lim_{E\to 0}\left(\frac{E}{Q(E)}\right). \tag{2}$$

We now introduce the effect of localized trapping states by writing the Shockley-Read-type balance equation [5] for the density of populated traps n_t,

$$\frac{dn_t}{dt} = c_t(N_t - n_t)n - \gamma n_t . \tag{3}$$

Here N_t is the total density of traps, and c_t and γ are the trapping coefficient and detrapping rate, respectively. By definition $c_t N_t \equiv \Gamma$ is the trapping rate by empty traps. While in semiconductors the Shockley-Read equation describes trapping of an electron (hole) by a discrete level as a localized trap in a superconductor is envisaged to contain a large number of states. Thus Eq. (3) deals with properly averaged quantities.

Detrapping occurs either directly via the absorption of a phonon or through recombination of the trapped qp with a free qp of high enough energy such that the resultant emitted phonon may break a Cooper pair and produce two free qp's. At temperatures normally used in experiments the latter process is dominant. Detrapping via recombination requires that the nonequilibrium qp's have, on average, an energy at least that of the trap depth above the superconducting edge Δ. We write the detrapping rate $\gamma(t) = R^+ n(t)$ with R^+ accounting for the events in which the recombination phonons are retained within the system, in contrast to R^* where they are lost from the structure, and also for those in which the excess qp's are too close to the superconducting edge to produce detrapping.

The overall trapping rate is constant as long as $N_t \gg n_t$ and if γ does not depend on qp density. These conditions are fulfilled for $E \to 0$. However, at high incident photon energy and specifically for the high quality STJ's now available, the number of excess qp's can approach or exceed the number of traps, therefore reducing the overall trapping rate and enhancing the detrapping process. We have generalized the RT equations to include the kinetics of trapped qp's as follows.

First, we solve (3) for $n_t(t)$, assuming all traps are empty at time $t = 0$. Then we split the loss term $\Gamma_{QL,j} n_j$ of (1) into the sum of a diffusive contribution $\tilde{\Gamma} n_j$ and a trap contribution $-\frac{dn_t}{dt}$ and introduce dimensionless qp densities $y(t) = \frac{n_1(t)}{n_0}$ and $z(t) = \frac{n_2(t)}{n_0}$ with n_0 being the initial qp density. We consider a symmetrical STJ, where all parameters are the same for both electrodes. Substituting $\frac{dn_t}{dt}$ into (1) with the symbols $\alpha = R^* n_0$, $\beta = \frac{n_T}{n_0} + \frac{\tilde{\Gamma}}{2\alpha}$, and $\zeta = (c_t + R^+)n_0$ leads to a new set of equations which replace (1),

$$\begin{aligned}\frac{dy}{dt} &= -\alpha(y^2 + 2\beta y) - \Gamma y \exp\left[-\zeta \int_0^t y(t')\,dt'\right] \\ &\quad - \Gamma_t(y - z) - \Gamma_{QPL,12} + \Gamma_{QPL,21} z , \\ \frac{dz}{dt} &= -\alpha(z^2 + 2\beta z) - \Gamma z \exp\left[-\zeta \int_0^t z(t')\,dt'\right] \\ &\quad - \Gamma_t(z - y) - \Gamma_{QPL,21} + \Gamma_{QPL,12} y .\end{aligned} \tag{4}$$

Analytical solution for multiple tunneling systems.—As will be discussed in the following section, the above equations may be solved numerically for an arbitrary set of parameters. Figure 1 shows the modeled responsivity for a typical sample. However, many of the salient features may be derived analytically by considering the limiting behavior of a multiple tunneling system. In this situation each qp on average tunnels several times before it is lost, i.e., $\Gamma_t \gg \max(\alpha, \Gamma_{QPL}, \tilde{\Gamma}, \Gamma)$. Under such circumstances the qp's become equally distributed between both electrodes before any loss occurs. Hence, the initial conditions can be taken as $y(t = 0) = z(t = 0) = \frac{1}{2}$ and at any instance of time $y(t) \simeq z(t) \simeq \frac{y(t)+z(t)}{2}$. Hence (4) can be reduced to a single equation for $y(t)$ [or $z(t)$]. Introducing the new function $\varphi(t) = \exp[-\zeta \int_0^t y(t')\,dt']$, measuring t in units of Γ_t^{-1} and integrating the resulting second order differential equation once with the initial condition $\varphi'(0) = -\frac{\zeta}{2\Gamma_t}$, we obtain the exact result,

$$\begin{aligned}\frac{\Gamma_t}{2\beta\zeta}\varphi' &= -\left[1 + \frac{1}{4\beta} - \frac{\Gamma}{2\beta(\zeta - \alpha)}\right]\varphi^{1+(\alpha/\zeta)} + \varphi \\ &\quad - \frac{\Gamma}{2\beta(\zeta - \alpha)}\varphi^2 .\end{aligned} \tag{5}$$

Since $\frac{Q(E)}{E} = -\frac{2e\Gamma_t N_0}{\zeta E}\ln\varphi(\infty)$, where N_0 is the initial number of qp's, a knowledge of the full time dependence of $\varphi(t)$ is unnecessary. At $t \to \infty$ we have $\varphi' = -\zeta\varphi y \to 0$ because $\varphi(\infty)$ remains finite while $y \to 0$, so that (5) becomes

$$\left(1 + \chi E - \frac{b}{c}\right)X + \frac{b}{c}X^{c+1} = 1 , \tag{6}$$

where $\chi E = \frac{1}{4\beta}$, $b = \frac{\Gamma}{2\beta\alpha}$, $c = \frac{\zeta}{\alpha} - 1$, and $X = [\varphi(\infty)]^{1/(c+1)}$. Note that b is primarily governed by the trapping rate Γ, while c contains both trapping (c_t) and detrapping (R^+) coefficients. The number of traps N_t influences only b. χ is mainly determined by the diffusive losses $\tilde{\Gamma}$.

At $E \to 0$ we obtain

$$\lim_{E\to 0}\frac{Q(E)}{E} = \frac{e}{1.75\Delta}\frac{\Gamma_t}{\Gamma + \tilde{\Gamma} + 2R^* n_T} . \tag{7}$$

Using (7) and (2) we arrive at the general expression,

$$S(E) = -(b + 1)\frac{\ln X}{\chi E}. \quad (8)$$

As follows from Eq. (7) at low photon energy the STJ responsivity is essentially constant. Simple analysis shows that it rises significantly when the photon energy exceeds a certain threshold, then saturates and then gradually decreases at high energies as $\frac{\ln(1+\chi E)}{E}$ due to the self-recombination process. The maximum value of responsivity occurs at an energy E_M obtained from setting the differential of $S(E)$ to zero and using (5) and (6). It is given by

$$S_M = \frac{b + 1}{bX_M^{c+1} + 1} X_M. \quad (9)$$

Thus the shape of the responsivity curve versus energy is determined primarily by the two parameters b and c. It will be of particular interest to determine the relative values of c_t and R^+, which appear combined in c. Thus $c_t \gg R^+$ implies a limited number of traps, while the opposite case $c_t \ll R^+$ describes the situation of a much higher density of traps, but with effective detrapping.

A strong nonlinearity of the STJ response results from either scenario. In the former case the sharp rise of the responsivity is the result of trap saturation, while in the latter it is the effective depopulation of the traps which makes such traps inefficient as a qp loss mechanism. Both mechanisms result in an increase of the qp lifetime such that the remaining free qp's carry on tunneling and contributing to the STJ response. With a further increase in qp density the responsivity saturates since the self-recombination becomes dominant and eventually causes its decrease as $\frac{\ln E}{E}$. The second mechanism described above can be considered as self-heating since the traps are effectively depopulated or heated up. In systems with multiple tunneling, after each tunneling event the qp emerges with an excess energy eV_b, where V_b is a bias voltage, so that the qp distribution is raised in energy above Δ. If the bias voltage is large enough, the number of tunnels per qp is large such that the mean qp energy is high. In this situation the depopulation factor R^+ may be close to the absolute recombination factor R, thus favoring self-heating.

Comparison with experiment.—Using the above equations, we have modeled the responsivity of a Nb-Al-AlO_x-Al-Nb STJ, in the range 1 to 6000 eV as shown in Fig. 1. This type of STJ is fully described in [2]. The device is diamond shaped, $20 \times 20\ \mu m^2$ deposited epitaxially on polished sapphire. The Nb and Al layers are 100 and 120 nm thick respectively, both for the top and the base film. The residual resistance ratio of the epitaxial base Nb film is ~70 and that of the polycrystalline top film is ~5. The AlO_x barrier has an estimated thickness of ≤ 1 nm and a resistance of $\sim 2.2 \times 10^{-6}\ \Omega \cdot cm^2$. The band gap of the device is 0.44 meV. In the range 40–2000 eV, the device was irradiated using monochromatic synchrotron radiation. It was installed in a He^3 cryostat at a temperature of ~320 mK with the chip mounted so as to fully illuminate the top electrode. It was biased at 0.18 mV. A magnetic field of ~8 mT was applied parallel to the junction in order to suppress the Josephson current and the Fiske steps.

Measurements in the optical range (1 to 5 eV) and at 6 keV were performed at 300 mK in a separate experiment [2], leading to a signal of ~2750 electrons per 1 eV in the optical and ~14 400 electrons per 1 eV at 6 keV. These results are consistent with the synchrotron data. The whole set is shown in Fig. 1 (crosses, +), with a maximum responsivity $S_M \sim 43.4$ at ~525 eV.

In order to fit the data, a numerical code was developed to solve Eqs. (3) and (4) with extra terms accounting for the qp diffusion from the absorption site. Parameters b and c are first estimated from the experimental results, using the analytical solutions described in the previous section. Equations (3) and (4) are then solved numerically using these values and the input parameters tuned to achieve a more accurate fit to the observations. Parameter χ may be determined independently, by noting that at maximum responsivity the signal decay is mostly controlled by residual losses. At 525 eV the measured time is 47 μs, giving $\tilde{\Gamma} \lesssim 2 \times 10^4\ s^{-1}$, hence χ.

Other parameters are the thermal population n_T and the recombination coefficients R, R^*, and R^+. Using the densities of states for qp's and Cooper pairs from the proximity effect model [6] and applying the general expression for the recombination rate given in [7] to the thermal population, one has $n_T \simeq 0.0827\ qp/\mu m^3$, and $R \simeq 600\ \mu m^3/s$ for qp's close to the energy gap Δ; for qp's of energy $\sim 1.25\Delta$, $R \sim 1200\ \mu m^3/s$. The proximity effect model of [6] was extended to the case of arbitrary layer thicknesses, to account for relatively thick Al layers. The effective recombination coefficient is given by $R^* = R(1 + \frac{\tau_{PL}}{\tau_{PB}})^{-1}$, with τ_{PL} the phonon escape time out of the electrode and τ_{PB} the Cooper pair breaking time for the phonons, calculated to be $\simeq$100 ps by averaging the characteristic times in Nb and Al over the density of states. The credibility of the proximity effect model on which our calculations for Γ_t, R, and τ_{PB} are based is supported by independent measurements of I-V curves, gap energy, and critical current versus temperature. The phonon loss time for Nb-based junctions similar to the device reported here has been empirically determined in [4] as ~1.2 ns, giving $R^* \simeq 46\ \mu m^3/s$ at the energy gap. Finally, R^+ is given by $\eta R(1 + \frac{\tau_{PB}}{\tau_{PL}})^{-1}$, where $\eta \leq 1$ accounts for the availability of only a fixed fraction of the excess qp's for detrapping. If $\eta = 1$, one has $R^+ \sim 510\ \mu m^3/s$. Allowing $600 < R < 1200\ \mu m^3/s$ and $10^4 < \tilde{\Gamma} < 2 \times 10^4\ s^{-1}$ leads to $0.018 < \chi < 0.072\ eV^{-1}$.

Parameter b can be estimated using Eq. (9) or from experimental measurements of S_M. At optical energies only trapping loss Γ is of importance. Using 2 μs measured signal decay time at optical range yields $\Gamma \simeq 5 \times 10^5\ s^{-1}$. Finally, applying Eq. (6) to the maximum responsivity point, using the range specified for χ and the

TABLE I. Parameters used for the fit of Fig. 1. All quantities are defined in the text.

Γ_t^{-1} (ns)	c_t (μm^3/s)	N_t (st/μm^3)	$\tilde{\Gamma}^{-1}$ (μs)	τ_{PB} (ps)	R (μm^3/s)	η	D (cm^2/s)
87	203.5	2870	70	120	1200	0.18	2

estimate of b, one has $1.1 < c < 5.9$. The resultant best fit is given by the solid line in Fig. 1. The best fit parameters, listed in Table I, all lie within the estimated ranges. The fit matches the data with a standard deviation of 1.4%, with a slight discrepancy around the maximum. A value of 2 cm^2/s for D indicates that diffusion in the structure is rather slow. Faster diffusion would produce a flatter responsivity below 300 eV and a sharper rise towards the maximum. The tunnel time of 87 ns accounts for a response of 2750 electrons per eV at 1 eV, while the proximity effect model predicts a tunnel time of 90 ns at the band gap with a slow rise over the broad range of qp energies reaching 150 ns by 2.5Δ. This does not exclude the possibility that qp's have a finite distribution above Δ. Indeed the best fit value for R corresponds to the qp energy of 1.25Δ, while η is not negligibly small. Finally, we note that c_t and R^+ are very similar, implying that this specific device is in the intermediate range between the self-heating and trap saturation mechanisms.

Finally, since the theoretical model introduces trap behavior phenomenologically it describes the effect of local traps of any kind, for example, the locally suppressed gap regions which occur due to known effects of Nb oxidation [8,9]. However, the traps might also be more fundamental in origin, for example, due to crystallographic imperfections at grain boundaries, STJ edges, or Nb/Al interfaces. In the latter case the lateral fluctuations of the main mesoscopic parameters determining the specific characteristics of a proximity effect may easily provide extra localized traps.

In summary, we have derived the generalization of the Rothwarf-Taylor balance equations to incorporate the effects of localized trap kinetics. It has been shown that the population and depopulation of traps can lead to a strong nonlinearity of the STJ response. The theory is shown to agree well with experimental observations in Nb/Al based STJ. The observation of the spectral maximum in the STJ responsivity profile provides a direct method of determining the trap density.

[1] A. Peacock, P. Verhoeve, N. Rando, A. van Dordrecht, B. G. Taylor, C. Erd, M. A. C. Perryman, R. Venn, J. Howlett, D. I. Goldie, J. Lumley, and M. Wallis, Nature (London) **381**, 135 (1996).
[2] P. Verhoeve, N. Rando, A. Peacock, A. van Dordrecht, A. Poelaert, D. I. Goldie, and R. Venn, J. Appl. Phys. **83**, 6118 (1998).
[3] A. Rothwarf and B. N. Taylor, Phys. Rev. Lett. **19**, 27 (1967).
[4] P. Verhoeve, N. Rando, J. Verveer, A. Peacock, A. van Dordrecht, P. Videler, M. Bavdaz, D. J. Goldie, T. Lederer, F. Scholze, G. Ulm, and R. Venn, Phys. Rev. B **53**, 809 (1996).
[5] W. Shockley and W. T. Read, Phys. Rev. **87**, 835 (1952).
[6] A. Golubov, E. Houwman, J. Gijsbertsen, V. Krasnov, J. Flokstra, and H. Rogalla, Phys. Rev. B **51**, 1073 (1995).
[7] A. Golubov, E. Houwman, J. Gijsbertsen, J. Flokstra, H. Rogalla, J. le Grand, and P. de Korte, Phys. Rev. B **49**, 12 953 (1994).
[8] E. L. Wolf, J. Zasadzinski, J. W. Osmun, and G. B. Arnold, J. Low Temp. Phys. **40**, 19 (1980).
[9] J. Halbritter, Appl. Phys. A **43**, 1 (1987).